

Vibration characteristics of polymer-based Langevin transducers

Jiang Wu , Yosuke Mizuno  and Kentaro Nakamura 

Laboratory for Future Interdisciplinary Research of Science and Technology, Tokyo Institute of Technology, Yokohama 226-8503, Japan

E-mail: wujiang@sonic.pi.titech.ac.jp

Received 17 April 2018, revised 17 July 2018

Accepted for publication 23 July 2018

Published 6 August 2018



Abstract

Our previous studies demonstrated that some functional polymers could exhibit satisfactorily low mechanical loss in high-amplitude bending vibration in the ultrasonic frequency range. In this study, to explore further applications of these functional polymers in high-power ultrasonic transducers, we focus on Langevin transducers as they are most widely employed in industrial applications. The developed transducer has a sandwich structure: piezoelectric ceramic elements are clamped between two polymer cylindrical bodies with a metal screw. The vibration characteristics of the polymer-based Langevin transducers differ from the metal-based ones owing to the difference in the material constants. When working in the 1st-order longitudinal modes, the polymer-based transducers exhibit dumbbell-shaped deformations because of the higher stiffness of the metal screws. Their mechanical losses reach the maximal values on the vibrating bodies instead of the piezoelectric ceramic elements. Besides, when the strains on polymer vibrating bodies exceed certain values, there exist sharp reductions in mechanical quality factors (Q factors), which restrict the maximal vibration velocities of polymer-based transducers. The poly phenylene sulfide (PPS)-based transducer yields Q factors of 350 and its vibration velocity linearly increases to 1060 mm s^{-1} , comparable to the maximal values achievable on metal-based ones. These properties indicate the potential of PPS-based transducers for ultrasonic applications.

Keywords: Langevin-type transducer, vibration characteristics, poly phenylene sulfide, polymer

(Some figures may appear in colour only in the online journal)

1. Introduction

Langevin-type ultrasonic transducer is a fundamental component for various kinds of high-power ultrasonic applications, e.g. cleaning, machining, welding, food industry, and enhancement of chemical reaction [1–3]. Conventional Langevin-type ultrasonic transducers consist of metal vibrating bodies and piezoelectric ceramic elements. Owing to low densities, functional polymers are attractive candidate materials as vibrating bodies for reducing the weight of transducers [4]. Besides, since polymer components are directly fabricated via molding rather than machining, the production efficiencies of transducers, particularly those with complex structures, can be significantly improved [5]. A series of our previous studies showed that several functional polymers had the capability of exhibiting relatively low mechanical loss

under high-amplitude bending vibration [4, 6–10]. In this study, we employ these polymers to substitute the metals as the vibrating bodies of Langevin longitudinal transducers, and systematically investigated the vibration characteristics as they may differ from those of metal-based ones because of the great differences in the mechanical constants [7].

First, utilizing functional polymers as well as metals, we prepare several Langevin transducers with identical dimensions. Subsequently, taking poly butylene terephthalate (PBT)- and aluminum-based transducers as examples, we compare their differences in vibration characteristics, including electrical admittances, deformations, dissipated power distributions, mechanical quality factors (Q factors), and achievable maximum vibration velocities. Finally, we summarize the Q factors and maximal vibration velocities achievable on the tested transducers.

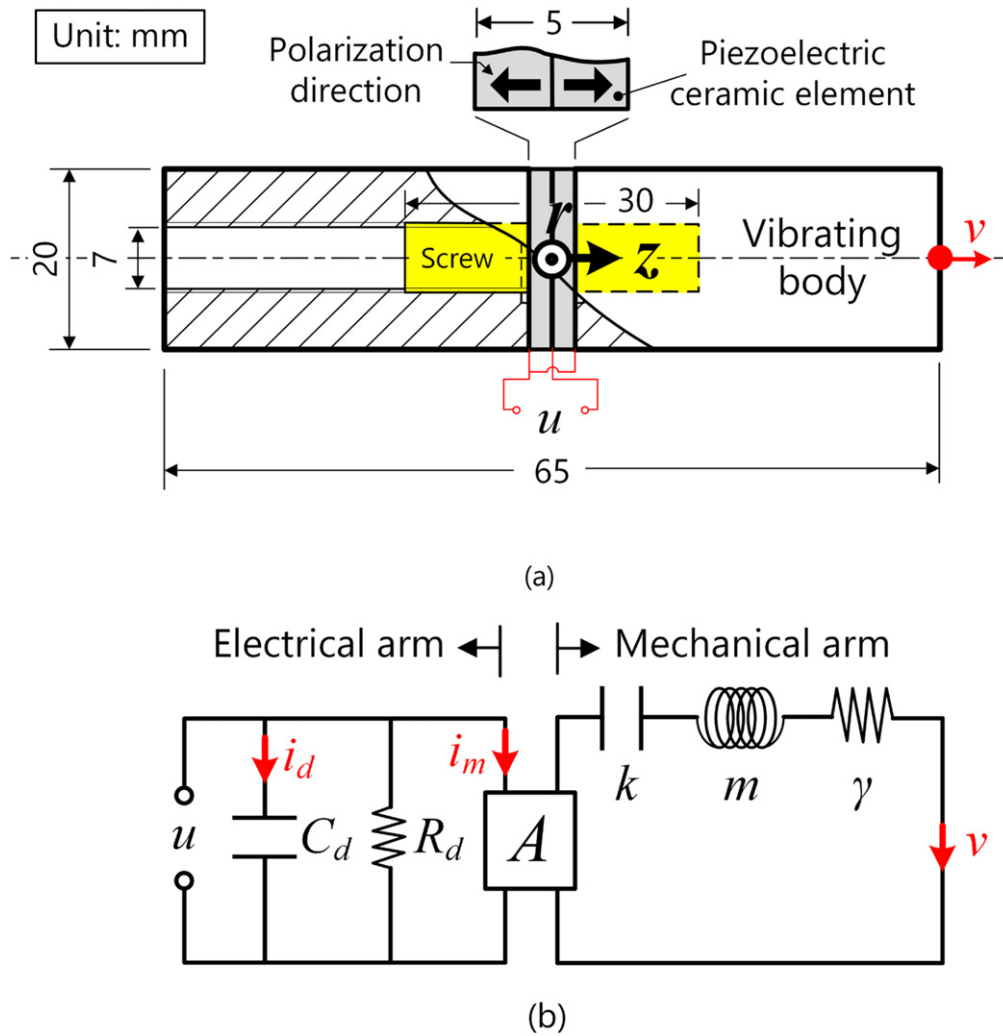


Figure 1. Langevin transducer tested in this study: (a) structure and (b) equivalent circuit model.

2. Langevin transducer and its equivalent circuit model

Figure 1(a) depicts the schematics of tested Langevin transducers. Two pieces of piezoelectric ceramic elements (C213, Fuji Ceramics, Fujinomiya, Japan) 8 and 20 mm in inner and outer diameters, respectively, and 2.5 mm in thickness are clamped by two cylindrical vibrating bodies with a 30 mm long screw. The 20 mm diameter vibrating bodies have through holes 7 mm in diameter and 30 mm in length. The tested transducers have identical dimensions but are made of different polymers and metals, of which the mechanical constants are listed in table 1 [11]. A polar coordinate is established on the middle surface of the transducer.

Figure 1(b) represents an equivalent circuit model for evaluating piezoelectric transducers [1, 12]: it comprises an electrical arm and a mechanical arm coupled by a force factor A . In the electrical arm, the clamped capacitance C_d and the dielectric loss R_d are parallelly connected. i_d and i_m denote the reactive current flowing into C_d and the motional current into A , respectively. In general, R_d is so large (in the order of $M\Omega$) that the current flowing into R_d is negligibly small [1, 10].

The mechanical arm contains three serially connected components, namely the equivalent stiffness k , mass m , and damper γ . v denotes the z -axis vibration velocity on the end surface of the transducer.

3. Experimental results

3.1. Experimental setup

Figure 2 illustrates the experimental setup. When a sinusoidal voltage is applied to transducer, the 1st longitudinal vibration is excited. Here, an in-plane laser Doppler vibrometer (IPV100, Polytec, Waldbronn, Germany) mounted on a linear guide rail was employed to measure the z -axis vibration velocity distribution along the axial direction. The amplitude and phase were recorded by a lock-in voltmeter (5560, NF Electronic Instruments, Yokohama, Japan). To know the z -axis vibration velocity on the lateral surface, we measured the in-plane vibration velocity on the cylindrical side surface close to the edge. Using a high frequency power meter (3332, Hioki E. E. Corp., Nagano, Japan), the voltage u and the input power p were measured. The motional current i_m was

Table 1. Material constants of tested materials [11].

| | Crystallinity | Polymer | Abbreviation | Material constants | | | |
|-------------------------|------------------|---------------------------|--------------|-----------------------|---|-----------------|---|
| | | | | Young's modulus (GPa) | Density ($\times 10^3 \text{ kg m}^{-3}$) | Poisson's ratio | Longitudinal wave speed in thin rod (m s^{-1}) |
| Thermal plastic | Semi-crystalline | Poly phenylene sulfide | PPS | 3.45 | 1.35 | 0.36 | 1599 |
| | | Poly ether sulfone | PES | 2.55 | 1.37 | 0.35 | 1364 |
| | | Poly ether ether ketone | PEEK | 3.50 | 1.32 | 0.40 | 1628 |
| | | Poly butylene terehtalate | PBT | 2.90 | 1.19 | 0.35 | 1473 |
| | | Poly oxy methylene | POM | 3.20 | 1.41 | 0.35 | 1506 |
| | | Poly methyl methacrylate | PMMA | 3.20 | 1.18 | 0.35 | 1633 |
| | | Polyamide 6 | PA6 | 2.60 | 1.14 | 0.35 | 1510 |
| | Amorphous | Poly ether imide | PEI | 3.00 | 1.27 | 0.37 | 1537 |
| Thermal setting plastic | — | Phenol formaldehyde resin | PF | 11.70 | 1.46 | 0.38 | 2831 |
| Metal | — | Aluminum | — | 70.30 | 2.70 | 0.35 | 5103 |

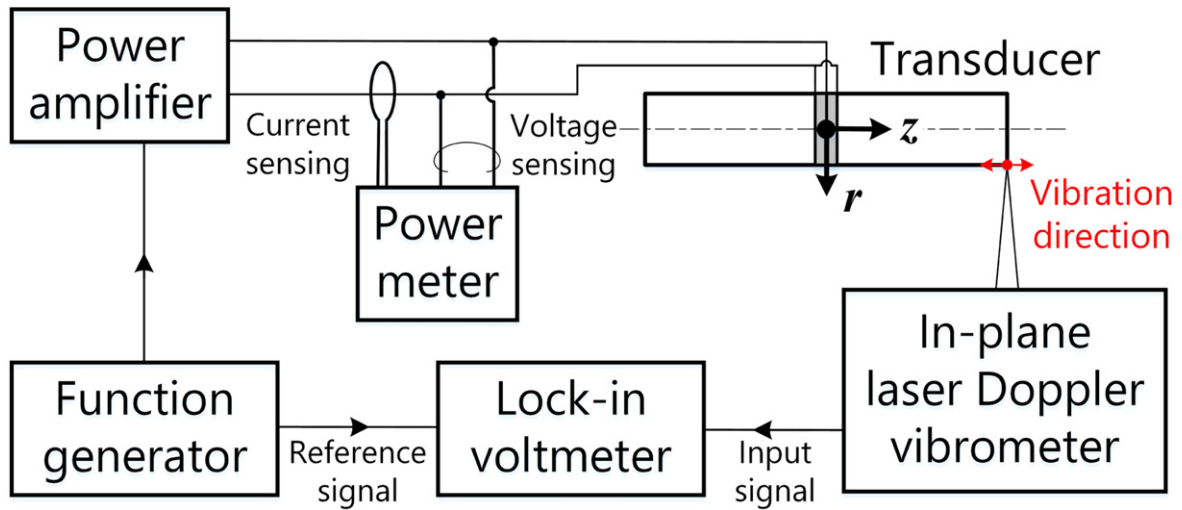


Figure 2. Testbed for measuring the vibration characteristics of transducers.

calculated as

$$i_m = \frac{2p}{u}. \quad (1)$$

Here, u , i_m , and v are indicated as the zero-to-peak values.

3.2. Electrical admittance

First, the electrical admittances of the PBT- and aluminum-based transducer were measured with an impedance analyzer (4294A, Agilent, Santa Clara, USA). In the admittance of the PBT-based transducer shown in figure 3(a), there was a resonance response at 14.1 kHz. The admittance loop shown in figure 3(b) shows that the susceptance is much higher than the conductance; this indicates that the mechanical vibration energy is far lower than the electrically stored energy. Figure 3(c) shows the admittance of the aluminum-based transducer. At 38.5 kHz, there existed an observable response. Figure 3(d) demonstrates that the motional admittance of the aluminum-based transducer was 12.5 mS, over 1000 times the value of the PBT-based one. In this case, the current dominantly flows into the mechanical arm. Table 2 gives the equivalent circuit parameters of these two transducers. The force factor is lower for the polymer-than for the aluminum-based transducer because of lower Young's moduli and lower densities of polymers [7]. Though the polymer-based transducer exhibits relatively low equivalent stiffness and mass, its damper is relatively high owing to the relatively low Q factor (see section 3.4). The low force factor and the high damper of the PBT-based transducer lead to the weak mechanical resonance [13].

3.3. Deformation and dissipated power

Subsequently, the deformations of the PBT- and aluminum-based transducers operated in the 1st-order longitudinal modes were investigated via finite element analysis (FEA). The model was meshed into several thousands of cuboid elements with sizes of 0.5 mm. The simulated resonance frequencies of the PBT- and aluminum-based transducers

were 14.6 and 39.5 kHz, respectively, slightly higher than those obtained from the admittance characteristics. It often occurred because of the mesh size and the modeling of the contacting area. Figure 4(a) illustrates that the PBT-based transducer exhibits a dumbbell-shaped deformation, different from that of the aluminum one shown in figure 4(b). Figures 4(c) and (d) show the z -axis vibration velocity distributions of the PBT- and aluminum-based transducers, respectively. It can be observed that the z -axis vibration velocity distribution of the PBT-based transducer deviates from the cosine waveform. The strain distribution shown in figure 5(a) was derived from the FEA results. The strain reached the maximal values at $z = -12$ and 12 mm, close to the lateral surfaces of the screw (at $z = -15$ and 15 mm), probably because of higher stiffness of the aluminum screw. On the basis of the vibration velocity distribution, the local dissipated power was estimated by the method given in appendix. As figure 5(b) shows, since there exist measurement errors caused by the non-uniformities in materials [14–17], we draw the envelopes to clearly illustrate the dissipated power distribution. The dissipated powers reach their maximal values at $z = -15$ and 19 mm, where the transducers exhibit higher strains. The temperature on the surface of the PBT-based transducer was measured with an infrared camera (i7, FLIR Systems, Wilsonville, USA) after it was continuously excited for approximately 5 min. Figure 5(c) demonstrates that the polymer vibrating bodies exhibit relatively high temperature compared to piezoelectric ceramic elements. The local dissipated powers near $z = -10$ and 10 mm are relatively low compared to the values near $z = -15$ and 19 mm, but these regions have almost the same temperatures. In addition to the mechanical loss, there exists frictional loss on the thread ridges between vibrating bodies and screws; that leads to the temperature rises near $z = -10$ and 10 mm [18]. The distributions of the vibration velocity and strain, dissipated power, and temperature on the surface of the aluminum-based transducer are illustrated in figures 5(d)–(f), respectively. Note that the temperature shown in figure 5(f) were measured after a 10 min continuous

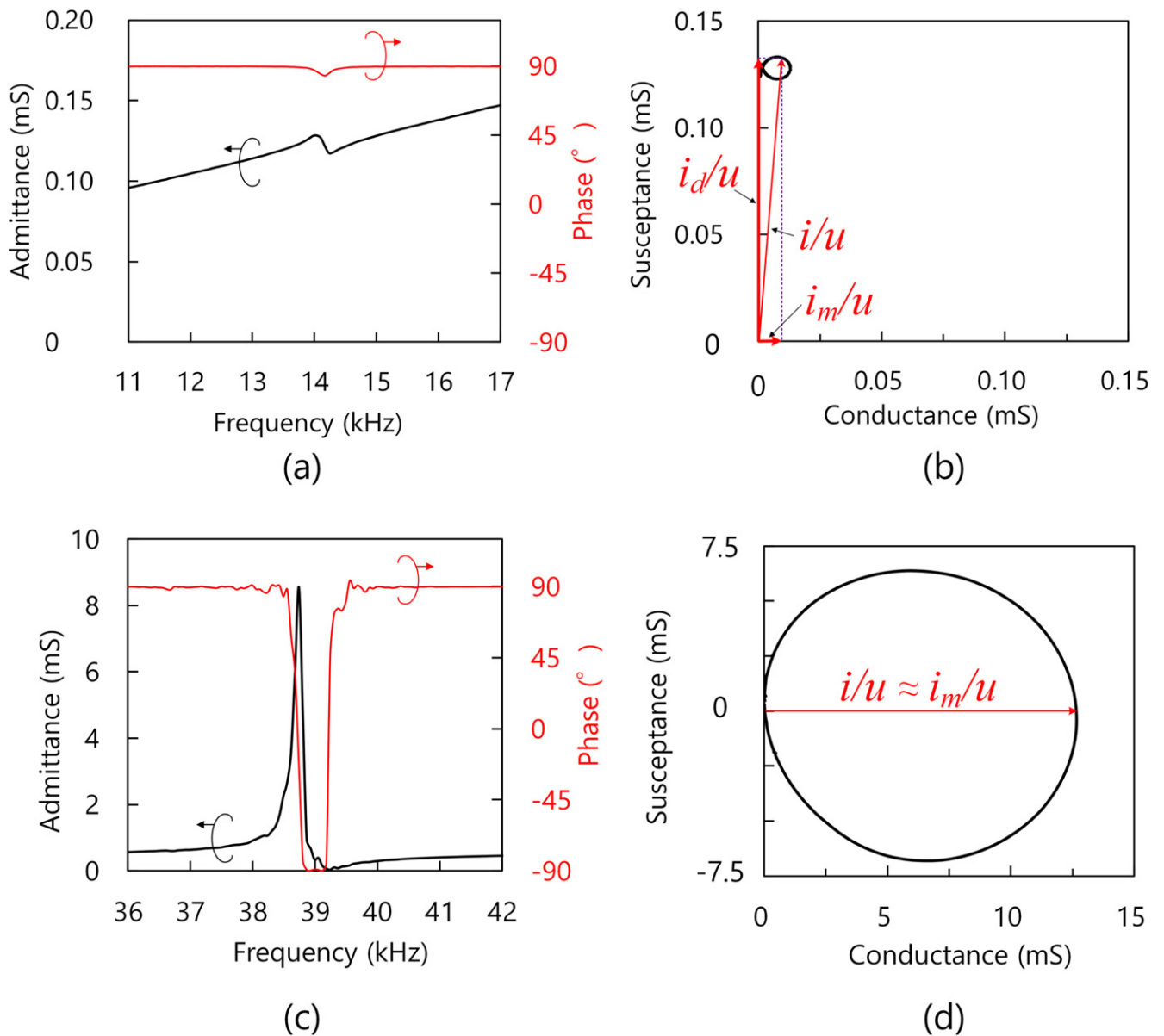


Figure 3. (a) Admittance characteristics of PBT-based transducer and (b) its admittance loop near 14.4 kHz. (c) Admittance characteristics of aluminum-based transducer and (d) its admittance loop near 38.5 kHz.

Table 2. Measured values of equivalent circuit parameters of PBT- and aluminum-based transducers.

| Material | Clamped capacitance C_d (nF) | Force factor A (N V^{-1}) | Equivalent stiffness k (10^6 N m^{-1}) | Equivalent mass m (10^{-3} kg) | Damper γ (N s m^{-1}) |
|----------|-----------------------------------|---|---|---|--|
| PBT | 2.11 | 0.012 | 76.4 | 9.3 | 12.2 |
| Aluminum | 2.05 | 0.133 | 647.2 | 11.4 | 1.4 |

excitation as the temperature rise was not observable in short time. Figure 5(e) demonstrates that higher power is dissipated in the piezoelectric ceramic elements (the part between $z = -2.5$ and 2.5 mm) than in the aluminum vibrating bodies. Since the piezoelectric ceramic elements have lower heat capacities and lower heat conductivity [19], they exhibit higher temperature rises than the aluminum vibrating bodies. During measurements, the vibration velocities on the end

surfaces of PBT- and aluminum-based transducers were respectively kept at approximately 60 and 100 mm s^{-1} ; and the measured power consumptions were 26.9 and 7.0 mW, respectively. The sums of local dissipated powers were estimated to be 18.4 and 4.4 mW for the PBT- and aluminum-based transducers, respectively. The other powers are assumed to frictionally dissipate on the thread ridges between vibrating bodies and screws [18].

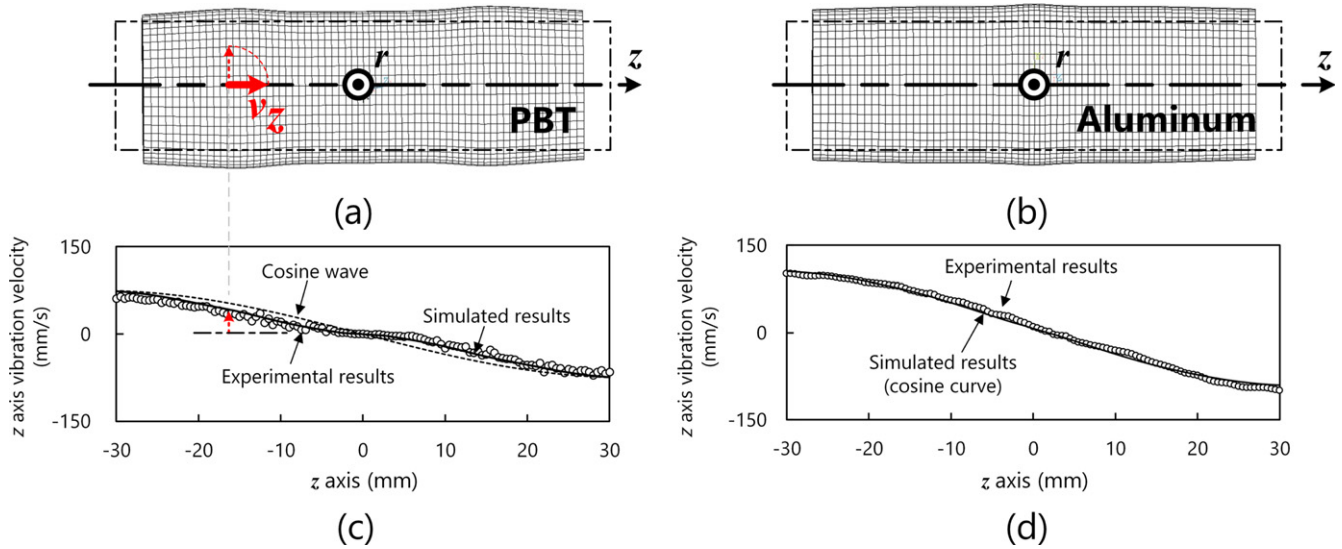


Figure 4. Vibration modes of (a) PBT-based and (b) aluminum-based transducers. In (c) and (d), the solid curves are their z -axis vibration velocity distributions obtained through FEA, and they agree with the experimental results (dots). Cosine waves (dashed curves) are given for comparison.

3.4. Q factor

Then, the resonance frequency and the Q factor were measured as functions of the vibration velocity. Here, the Q factors of the PBT-based transducer were obtained from the resonance frequency f_r and the bandwidth Δf corresponding to 0.707 times of the maximal vibration velocity [1, 4, 12]:

$$Q = \frac{f_r}{\Delta f}. \quad (2)$$

As shown in figure 6(a), the Q factor had almost no variation when the vibration velocity increased from 25 to 64 mm s^{-1} . However, it yielded a sharp reduction when the vibration velocity exceeded 64 mm s^{-1} . In the meantime, the resonance frequency decreased from 14.39 to 14.36 kHz. As shown in figure 6(b), the Q factors of the aluminum-based transducer in low-amplitude region ($< 800 \text{ mm s}^{-1}$) were also calculated from the resonance curves. On the other hand, the Q factors in high-amplitude region were estimated from the transient response to avoid the effect caused by the temperature rise [20–22]. The vibration velocity dependence of Q factor of the aluminum-based transducer provided the similar tendency with that of the PBT-based one. At the vibration velocity of 1500 mm s^{-1} , the maximal strains on both the aluminum vibrating body and the piezoelectric ceramic element reached 0.029%. In general, Q factors of transducers reflect the mechanical losses of component materials. According to the previous reports [16, 20], the Q factors of aluminum and piezoelectric ceramics sharply decrease at the strains of 0.060% and 0.027%, respectively. Thus, the significant Q factor reduction of the aluminum-based transducer at over 1500 mm s^{-1} originates from the sharp increase in the mechanical loss of the piezoelectric ceramic elements [16, 22]. In the case of the PBT-based transducer, the strain on the vibrating body was approximately 0.004% at 64 mm s^{-1} . Figure 7 shows the strain dependences of Q

factors of several polymer materials measured by our developed method [17]. Clearly, when the strain on the polymer vibrating body exceeds 0.004%, the Q factor of PBT decreases by approximately 70. Whereas the strain is 0.001% on the piezoelectric ceramic element; this value is far lower than the value corresponding to the rapid Q factor reduction (0.027%). Clearly, the large increase in mechanical loss of the polymer vibrating body causes the sharp reduction in the Q factor of the entire transducer. Figure 8 demonstrates how the Q factors of transducers made of other polymer materials depend on their vibration velocities. The maximal Q factors of POM-, PBT-, and PMMA-based transducers were respectively 42, 71, and 47, limited by the Q factors of POM, PBT, and PMMA (respectively 60, 90, and 70; see figure 7). Note that since the Q factor of a material Q_{mat} excludes the mechanical loss on contact surfaces between vibrating bodies and piezoelectric ceramic elements, as well as those on thread ridges, it is higher than the Q factor of the transducer made of the material. The maximal vibration velocities of POM- and PMMA-based transducers can be linearly increased to 60 and 100 mm s^{-1} , respectively, corresponding to the strains where the Q factors of POM and PMMA sharply decrease (respectively 0.003% and 0.006%; see figure 7). These results validate our aforementioned conclusion. Besides, the transducers made of semi-crystalline polymers, e.g. PPS and PEEK, exhibited relatively high Q factors compared to that of the amorphous polymer except the PA6-based transducer with a Q factor of lower than 10. The PPS-based Langevin-type transducer yielded Q factors of approximately 350; this high value originates from low mechanical loss of PPS [6]. Another transducer capable of exhibiting Q factors of higher than 100 was made of PES. Interestingly, both PPS and PES are sulfur compounds [11].

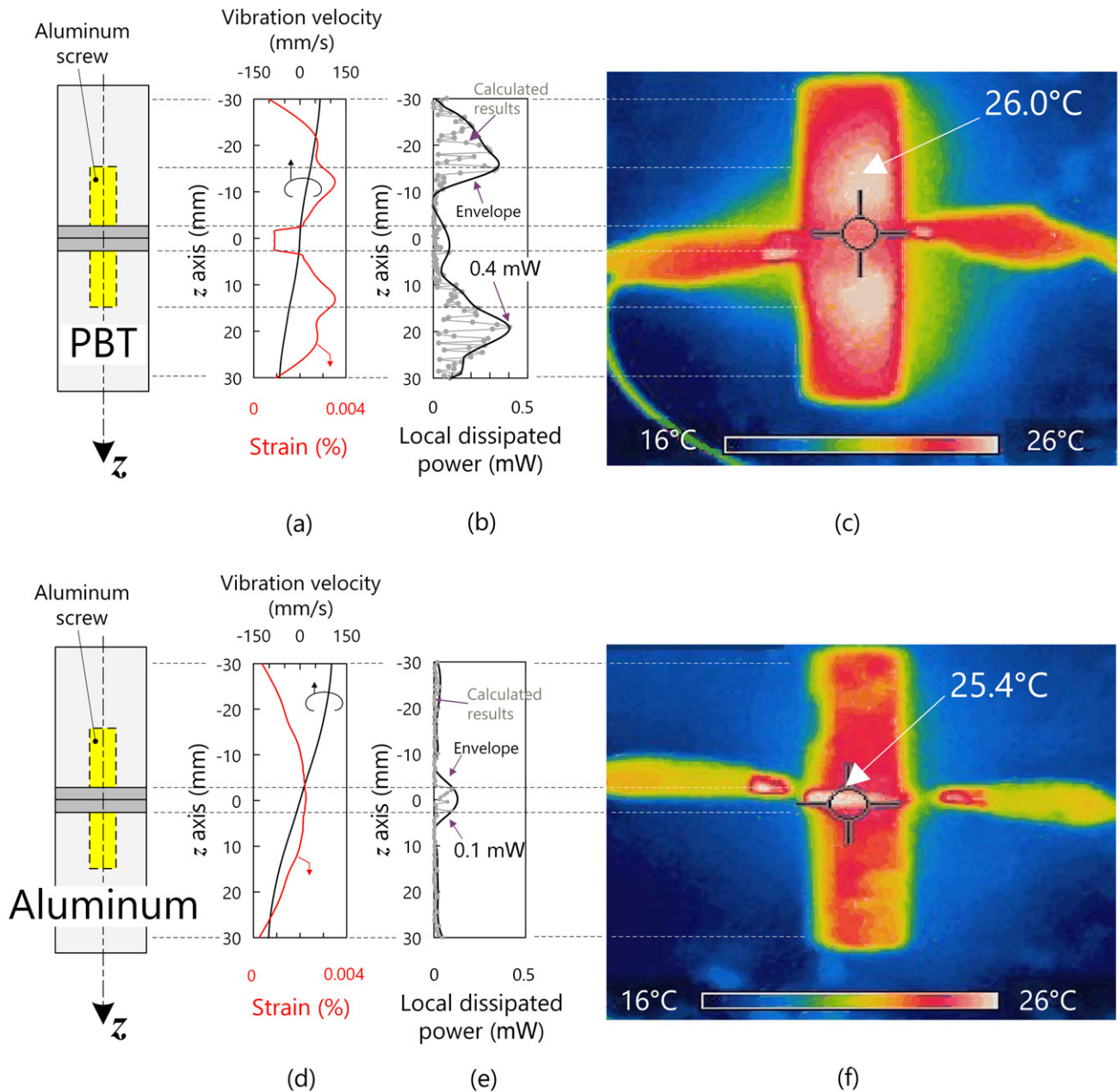


Figure 5. Strains (red curves) of (a) PBT- and (d) aluminum-based transducers derived from the simulated vibration velocities (black curves). Local dissipated powers of (b) PBT- and (e) aluminum-based transducers. The gray curves are the estimated local dissipated powers, and the black curves are their envelopes. (c) and (f) respectively show the temperature distributions on the surfaces of the PBT- and aluminum-based transducers.

3.5. Achievable maximum vibration velocity

Finally, we investigate how linearly the vibration velocity v increased as the motional current i_m becomes higher. As shown in figure 9(a), initially, the vibration velocity of the PBT-based transducer linearly increased to 64 mm s^{-1} . Then, in the i_m range from 0.9 to 1.7 mA, the vibration velocity had a nonlinear increase. At 1.7 mA, the vibration velocity approached its saturated value, 104 mm s^{-1} . The vibration velocity of the aluminum-based transducer shown in figure 9(b) has the similar tendency. As mentioned above, the vibration velocity can be linearly increased until the Q factor of material provides a marked reduction. The saturation in

vibration velocity probably originates from the nonlinearity in Young's modulus in high-amplitude region [23]. For practical applications of polymers in Langevin transducers in the future, two important indicators for practical applications, i.e. maximal vibration velocities in linear regions v_l and the saturated vibration velocities v_s of the tested transducers, are summarized in table 3. In contrast to most of the polymer-based transducers incapable of providing the performance comparable to metal-based ones dominantly owing to their low Q factors, the PPS-based transducer yields a maximal vibration velocity of 1060 mm s^{-1} in linear region. Considering its satisfactorily high vibration velocity and chemical

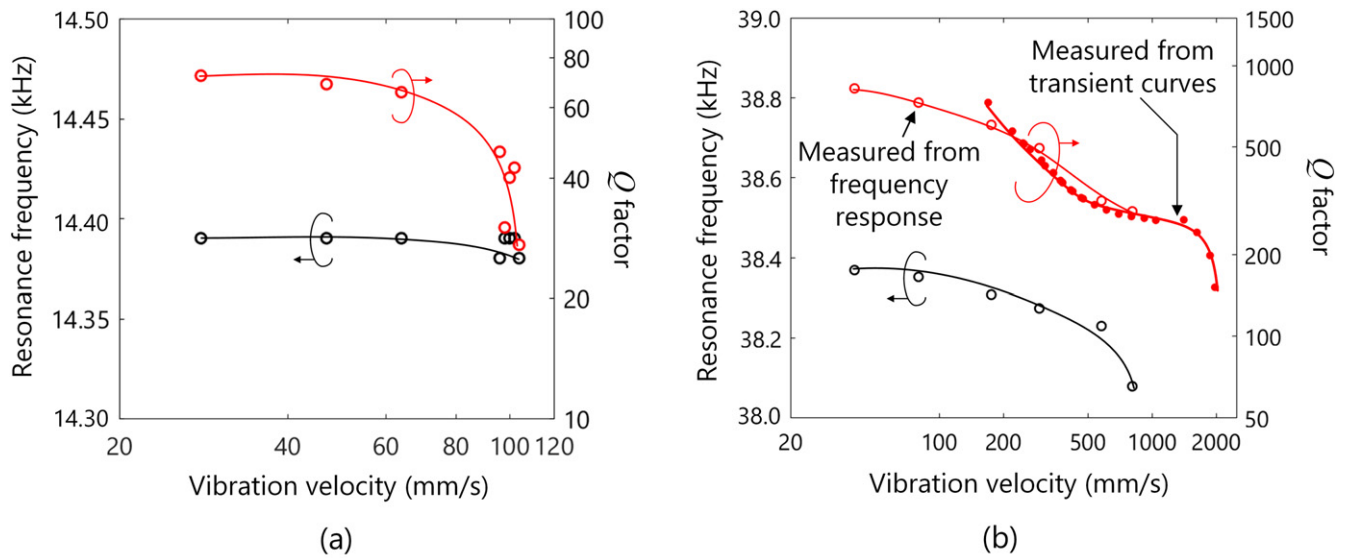


Figure 6. Resonance frequencies (black curves) and Q factors (red curves) as functions of the vibration velocities of (a) PBT- and (b) aluminum-based transducers. The open and closed bullets represent the results measured from the frequency response and the transient curve, respectively.

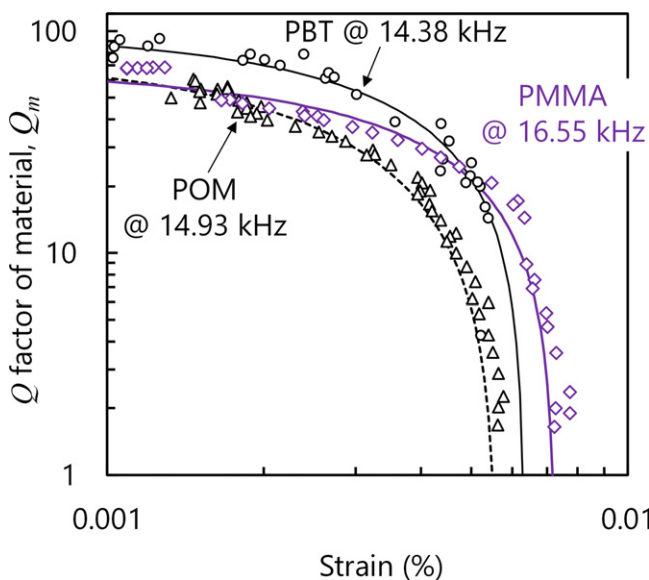


Figure 7. Variations in Q factors of PBT, POM, and PMMA against strains.

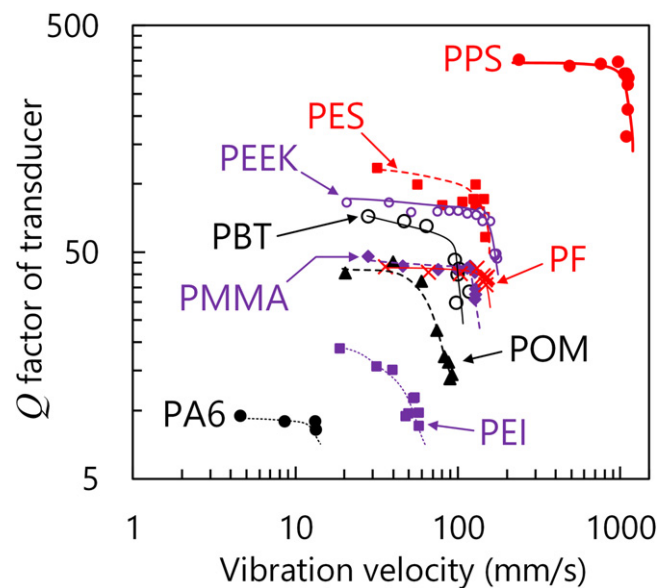


Figure 8. Q factors of transducers as functions of the vibration velocities on the end surfaces.

resistance, it is possibly applicable in special circumstances. For instance, PPS-based transducers can generate ultrasounds into acid or alkaline solutions to enhance chemical reactions, or be utilized as sensors for robots used in chemical plants [24].

4. Conclusions

After carrying out a systematical investigation on the vibration characteristics of polymer-based Langevin transducers, we have drawn the following conclusions:

1. The mechanical loss of polymer-based Langevin transducers reached their maximal values on vibrating bodies rather than piezoelectric ceramic elements. Whereas conventional metal-based ones exhibited their maximal mechanical loss on the piezoelectric ceramic elements.
2. When the strain exceeded a certain value, the polymer-based transducer exhibited a sharp reduction in Q factor, which originated from the sharp increase in the mechanical loss of the polymer vibrating body. The attainable maximum vibration velocity of the transducer depended on the characteristics of each polymer material.

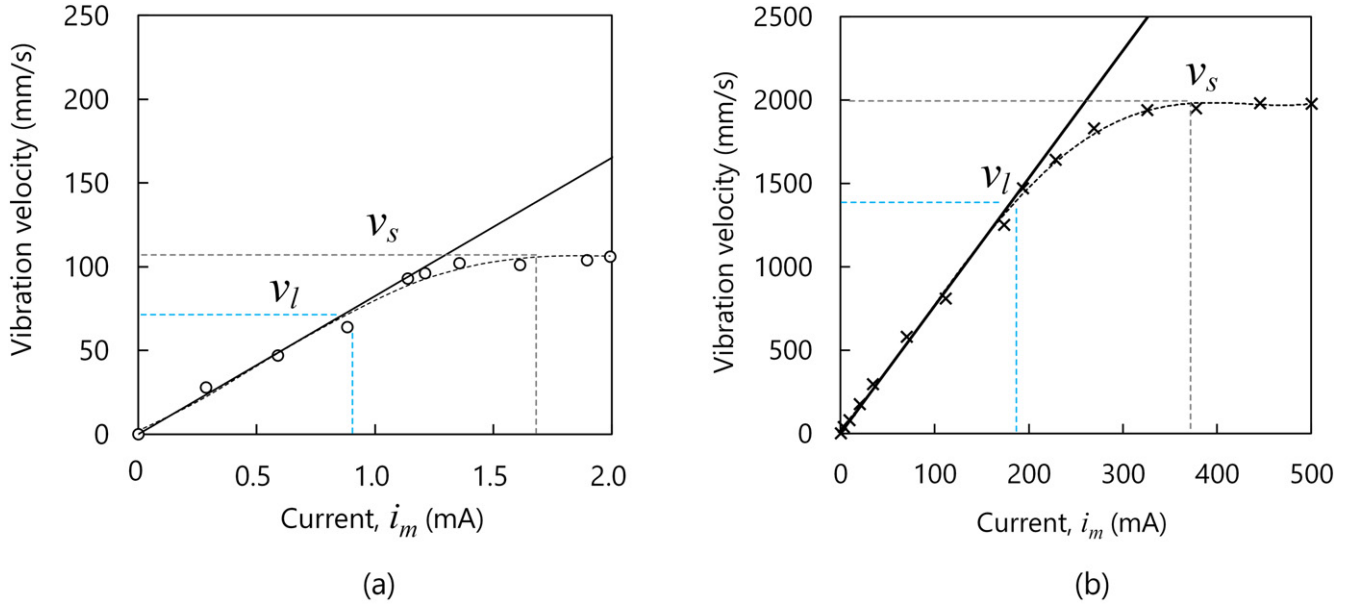


Figure 9. Vibration velocities as functions of the motional currents of (a) PBT- and (b) aluminum-based transducers.

Table 3. Maximal vibration velocities in linear region and saturated vibration velocities of transducers made of different materials.

| Material | Maximal vibration velocity in linear region, v_l (mm s^{-1}) | Saturated vibration velocity, v_s (mm s^{-1}) |
|----------|---|--|
| PPS | 1060 | 1120 |
| PES | 108 | 148 |
| PEEK | 116 | 179 |
| PBT | 64 | 104 |
| POM | 60 | 94 |
| PMMA | 100 | 128 |
| PA6 | 9 | 13 |
| PEI | 32 | 58 |
| PF | 132 | 150 |
| Aluminum | 1400 | 2000 |

- Most of the tested polymer-based transducers yielded Q factors of lower than 100, except that the PPS- and PES-based transducers yielded Q factors of approximately 350 and 115, respectively.
- The vibration velocity of the PPS-based Langevin transducer linearly increased to 1060 mm s^{-1} .

We anticipate that these results will provide adequate information for further design of polymer-based transducers. Towards practical applications, other properties of polymer-based transducers, e.g. long-term durability, should be assessed. Usage of stiff polymers, e.g. carbon- or glass-fiber-enhanced PPS/PEEK [4] and thermal annealing on polymers [17] are also worth exploring in the future.

Acknowledgments

The authors thank Daicel Corporation for providing various kinds of transducer components. This work was supported by

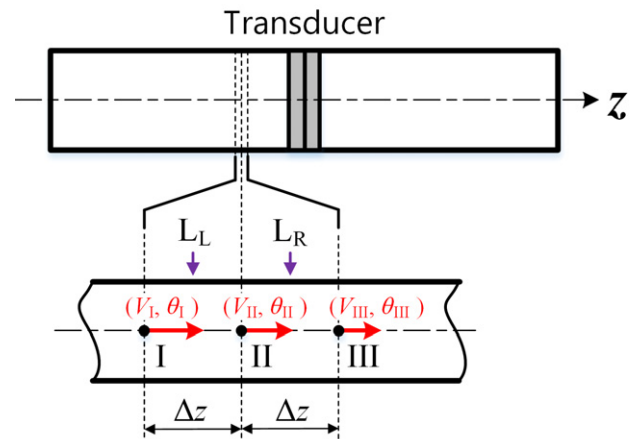


Figure A1. Conceptual view of calculation method of local dissipated power from longitudinal vibration velocity distribution on transducer surface.

JSPS KAKENHI Grant Number 17J05057 and JST A-step program Grant Number AS2711904S.

Appendix

As shown in figure A1, we assume three adjacent sampling points I, II, and III on the cylindrical vibrating body, and the cross-sections L_L and L_R in the middle of points I and II, and II and III, respectively. When the points I, II, and III respectively have the vibration velocities $v_I = V_I \exp(-j\theta_I)$, $v_{II} = V_{II} \exp(-j\theta_{II})$, and, $v_{III} = V_{III} \exp(-j\theta_{III})$, where V_i represents the amplitude and θ_i denotes the phase of the vibration velocity at the i th point ($i = I, II, \text{ and } III$), the active powers flowing into the small region between L_L and L_R are

given as [14]

$$P_L = \frac{ES}{2\omega\Delta z} \cdot V_I V_{II} \sin(\theta_I - \theta_{II}), \quad (\text{A-1})$$

where E denotes the Young's modulus, ω represents the angular frequency, Δz is the interval between the sampling points (=0.5 mm in this study), and S is the cross-sectional area. Similarly, the active power flowing out of the region is expressed as [14]

$$P_R = \frac{ES}{2\omega\Delta z} \cdot V_{II} V_{III} \sin(\theta_{II} - \theta_{III}). \quad (\text{A-2})$$

The power dissipated in this region is calculated as [6, 16]

$$P_{\text{dis}} = P_L - P_R. \quad (\text{A-3})$$

ORCID iDs

Jiang Wu  <https://orcid.org/0000-0002-6899-5601>

Yosuke Mizuno  <https://orcid.org/0000-0002-3362-4720>

Kentaro Nakamura  <https://orcid.org/0000-0003-2899-4484>

References

- [1] Nakamura K 2012 *Ultrasonic Transducers: Materials and Design for Sensors, Actuators, and Medical Applications* (Cambridge: Woodhead Publishing Limited)
- [2] Mason T J 1992 Industrial sonochemistry: potential and practicality *Ultrasonics* **30** 192–6
- [3] Naki T, Asami T and Miura H 2016 Convergence of intense aerial acoustic waves radiated by a rectangular transverse vibrating plate *Japan. J. Appl. Phys.* **55** 07KE09
- [4] Wu J, Mizuno Y, Tabaru M and Nakamura K 2015 Ultrasonic motors with polymer-based vibrators *IEEE Trans. Ultrason. Ferroelectr. Freq. Control* **62** 2169–78
- [5] Billiet T, Vandenhoute M, Schelfhout J, Vlierbergh S V and Dubruel P 2012 A review of trends and limitations in hydrogel-rapid prototyping for tissue engineering *Biomaterials* **33** 6020–41
- [6] Wu J, Mizuno Y, Tabaru M and Nakamura K 2016 Measurement of mechanical quality factors of polymers in flexural vibration for high-power ultrasonic application *Ultrasonics* **69** 74–82
- [7] Wu J, Mizuno Y and Nakamura K 2017 Structural parameter study on polymer-based ultrasonic motor *Smart Mater. Struct.* **26** 115022
- [8] Wu J, Mizuno Y, Tabaru M and Nakamura K 2016 Traveling wave ultrasonic motor using polymer-based vibrator *Japan. J. Appl. Phys.* **55** 018001
- [9] Wu J, Mizuno Y and Nakamura K 2018 Polymer-based ultrasonic motors utilizing high-order vibration modes *IEEE/ASME Trans. Mechatronics* **23** 788–99
- [10] Takagi K et al 1999 *Ultrasonic Handbook* (Tokyo, Japan: Maruzen Publication) (In Japanese)
- [11] Mark J E et al 1999 *Polymer Data Handbook* (New York: Oxford University Press)
- [12] Ley B F, Lutz S G and Rehberg C F 1959 *Linear Circuit Analysis* (New York: McGraw-Hill)
- [13] Liu Y, Chen W, Liu J and Yang X 2013 A high-power linear ultrasonic motor using bending vibration transducer *IEEE Tran. Ind. Electron.* **60** 5160–6
- [14] Morikawa R, Ueha S and Nakamura K 1996 Error evaluation of the structural intensity measured with a scanning laser Doppler vibrometer *J. Acoust. Soc. Am.* **99** 2913–21
- [15] Morikawa R, Nakamura K and Ueha S 1997 Measuring the structural intensity by sensing the in-plane vibration *J. Acoust. Soc. Technol.* **18** 201–3
- [16] Nakamura K, Kakihara K, Kawakami M and Ueha S 2000 Measuring vibration characteristics at large high amplitude region of material for high power ultrasonic vibration system *Ultrasonics* **38** 122–6
- [17] Wu J, Mizuno Y and Nakamura K 2017 Increasing in Q factor of poly phenylene sulfide at high-amplitude ultrasonic vibration by thermal annealing *Proc. Symp. Ultrason. Electron.* 1P1-8
- [18] Adachi K 2009 High-power ultrasonic transducers—a designing method for bolt-clamped Langevin-type transducers and its application *J. Japan. Soc. Precis. Eng.* **75** 479–83 (In Japanese)
- [19] Yarlaga S, Chan M H W, Lee H, Lesieutre G A, Jensen D W and Messer R S 1995 Low temperature thermal conductivity, heat capacity, and heat generation of PZT *J. Intell. Mater. Syst. Struct.* **6** 757–64
- [20] Umeda M, Nakamura K and Ueha S 1998 The measurement of high-power characteristics for a piezoelectric transducer based on electrical transient response *Japan. J. Appl. Phys.* **37** 5322–5
- [21] Umeda M, Hayano S and Takahashi S 2016 Nonlinear vibration for piezoelectric ceramic resonator *J. Acoust. Soc. Japan* **72** 228–33 (In Japanese)
- [22] Umeda M, Nakamura K and Ueha S 1999 Effects of vibration stress and temperatures on the characteristics of piezoelectric ceramics under high vibration amplitude levels measured by electrical transient responses *Japan. J. Appl. Phys.* **38** 5581–5
- [23] Iwama N, Miyake S and Morita T 2017 Modeling of Langevin transducer with transfer matrix of piezoelectric 33-mode introducing nonlinear elastic coefficients *IEICE Technical Report* US2017-81 (In Japanese)
- [24] Hill H. W. and Brady D. G 1976 Properties, environmental stability, and molding characteristics of poly phenylene sulfide *Polym. Eng. Sci.* **16** 831–5